CHINESE OPTICS LETTERS

Vol. 19, No. 5 | May 2021

Full-waveform fast correction method for photon counting Lidar

Ahui Hou (侯阿慧)[1,2*], Yihua Hu (胡以华)[1,2**], Nanxiang Zhao (赵楠翔)[1,2], Jiajie Fang (方佳节)[1,2], Shilong Xu (徐世龙)[1,2], and Quan Zhou (周 权)[1,2]

[1] State Key Laboratory of Pulsed Power Laser Technology, National University of Defense Technology, Hefei 230037, China

[2] Anhui Provincial Key Laboratory of Electronic Restriction, National University of Defense Technology, Hefei 230037, China

*Corresponding author: hou_a_hui068@163.com

**Corresponding author: skl_hyh@163.com

Received August 23, 2020 | Accepted October 29, 2020 | Posted Online February 20, 2021

The first photon bias of photon detection results in distortion of the photon waveform, which seriously affects the accurate acquisition of target information. A rapid universal recursive correction method is proposed, which is suitable for multi-trigger and single-trigger modes of photon detection. The calculation time is 2 to 3 orders of magnitude faster than that of Xu *et al.*'s method. In the experiment, we have obtained good correction results for area targets and targets with varying depths. When the average number of echo photons is 0.89, the correlation distance of the correction waveform is reduced by 85%.

Keywords: photon counting Lidar; waveform correction; waveform distortion; single pixel.

DOI: 10.3788/COL202119.052701

1. Introduction

Photon counting Lidar is widely used in target detection because of its high sensitivity and long detection range. Based on point-by-point scanning, a photon counting Lidar measures the flight time and the counts of photon events from a single pixel to achieve high-precision ranging[1,2] and three-dimensional imaging[3–12]. Given that the size of the laser spot at the target becomes larger with the increase of detection distance[12], extracting only one distance and reflectivity information from each pixel can no longer meet the needs of target detection and identification. It is well-known that the photon waveform, which is the statistical histogram from multiple cumulative detections of time-correlated single-photon counting (TCSPC)[13], has an internal relationship with the pulse laser[14–17]. The pulse laser echo is modulated by the target characteristics[18–20]. Therefore, the photon waveform is related to the characteristics of the target and can be used to obtain the target details. However, due to the existence of dead time, the first photon bias occurs[21], which results in distortion between the photon waveform and pulse laser waveform (viewed as the ideal waveform). As a result, the target detail information contained in the photon waveform is no longer accurate. Hou *et al.*[22] analyzed the relationship between distortion and dead time as well as system factors without performing waveform correction analysis. Therefore, it is of great significance to study the correction method of the photon waveform to restrain the distortion of the photon waveform and acquire accurate target details.

Based on the photon Poisson probability distribution, Oh *et al.*[23] proposed the walk error of photon ranging for the first time, to the best of our knowledge, and corrected it with the center of the mass detection method. He *et al.*[24] and Chen *et al.*[25] obtained the theoretical time error as compensation through simulation, so as to realize the correction of the range walk error. Huang *et al.*[26] deeply analyzed the influence of parameters on the walk error and corrected it. Xu *et al.*[27] proposed a new signal restoration method based on the Poisson probability response model and restrained the walk error with the center of the mass detection method. The above researches focus on the correction of the range walk error of the photon ranging and lack research focuses on the reconstruction and correction of the photon waveform itself. Based on the single-photon detection probability, Jonsson *et al.*[28] gave the reconstructed photon intensity distribution waveform and obtained the optimum range of detection probability for targets hidden in vegetation or camouflaged. Since the focus is on the detection probability of the target, the discussion of the waveform reconstruction of the intensity distribution is relatively simple. The summation form of the correction method severely slows down the data processing speed.

Here, we propose a fast and universal general recursive correction method for the photon waveform based on the

single-photon detection probability model, which is suitable for the multi-trigger and single-trigger modes. Subsequently, the calculation speed of our method is verified. After that, the effects of the photon waveform correction method with different intensities have been experimented and discussed. Finally, the photon waveform is corrected for the target with varying depths to verify the universality of the correction method.

2. Full-Waveform Correction Model

Following the theory of the Poisson probability response model[29–31], the detection probability of the time bin is

$$P_0(i) = 1 - \exp[-N(i)], \tag{1}$$

where $N(i)$ is the average number of photons in a time bin, $N(i) = N_s(i) + N_n$, $N_s(i)$ is the average number of echo photons, and N_n is the number of noise photons in a time bin.

Single-photon detectors have dead time. According to the length of the dead time and the range gate, photon detection can be divided into two modes[32]: single-trigger and multi-trigger. In the single-trigger mode, only one photon event can be detected during the range gate, and the detection probability of the ith time bin is

$$P(i) = \{1 - \exp[-N(i)]\} \cdot \exp\left[-\sum_{j=1}^{i-1} N(j)\right]. \tag{2}$$

Combining Eqs. (1) and (2), the correction function is defined as follows:

$$F_C(i) = \frac{P(i)}{P_0(i)} = \exp\left[-\sum_{j=1}^{i-1} N(j)\right],$$

$$F_C(i) = \{1 - 1 + \exp[-N(i-1)]\} \exp\left[-\sum_{j=1}^{i-2} N(j)\right]. \tag{3}$$

Thus, we can obtain the recursive correction function:

$$F_C(i) = F_C(i-1) - P(i-1). \tag{4}$$

In the multi-trigger mode, the dead time is less than the gate time, and multiple photon events can be detected within the gate time. The premise of detecting the ith time bin is that it cannot be triggered by any photon event within the previous dead time[33]:

$$P(i) = \{1 - \exp[-N(i)]\} \cdot \left[1 - \sum_{j=i-\text{dead}+1}^{i-1} P(j)\right]. \tag{5}$$

The correction function for the multi-trigger mode is

$$F_C(i) = \frac{P(i)}{P_0(i)} = 1 - \sum_{j=i-\text{dead}+1}^{i-1} P(j). \tag{6}$$

The correction function is expressed in recursive form:

$$F_C(i) = F_C(i-1) - P(i-1) + P(i - \text{dead}). \tag{7}$$

In summary, the correction function of the photon waveform is

$$F_C(i) = \begin{cases} F_C(i-1) - P(i-1), & i \le \text{dead} \\ F_C(i-1) - P(i-1) + P(i - \text{dead}), & i > \text{dead} \end{cases}, \tag{8}$$

when i is not equal to 1; otherwise, $F_C(1) = 1$.

In the time-of-arrival histogram of photons built up by multiple pulses, $P(i)$ can be expressed as $P(i) = K(i)/M$, where $K(i)$ is the count of photon events in the ith time bin, and M is the number of the emitted laser pulse.

The pulse laser waveform of the target can be restored:

$$N_s(i) = -\ln\left[1 - \frac{P(i)}{F_C(i)}\right] - N_n. \tag{9}$$

So far, based on the full-waveform correction method of photon counting Lidar, the rapid reconstruction and recovery of target laser echo have been achieved.

To accurately describe the overall difference between the photon waveform or the corrected waveform and the ideal waveform, the correlation distance R_C is defined as

$$R_C = 1 - \frac{\sum (\boldsymbol{W} - \overline{\boldsymbol{W}})(\boldsymbol{N}_{s0} - \overline{\boldsymbol{N}}_{s0})}{\sqrt{\sum (\boldsymbol{W} - \overline{\boldsymbol{W}})^2}\sqrt{\sum (\boldsymbol{N}_{s0} - \overline{\boldsymbol{N}}_{s0})^2}}, \tag{10}$$

where $\boldsymbol{N}_{s0}$ is the ideal waveform, and $\overline{\boldsymbol{N}}_{s0}$ is the mean of $\boldsymbol{N}_{s0}$; $\boldsymbol{W}$ is the photon waveform or the corrected waveform, and $\overline{\boldsymbol{W}}$ is its mean. The smaller the correlation distance, the lower the waveform distortion becomes, and the more similar the waveforms are.

Notably, if the number of photons is greater than 0.1[12], a big distortion will be introduced between the photon waveform and the ideal laser echo. Considering that there is a relationship between the detection probability and the original signal, the difference can be controlled.

The emitted laser with Gaussian distribution is given by

$$N_r(t) = \frac{N_s}{\sqrt{\pi}\tau} e^{-\frac{t^2}{\tau^2}}, \tag{11}$$

where N_s is the average number of photons in one signal period; $\tau = \text{FWHM}/(2\sqrt{\ln 2})$, and FWHM is the full width at half-maximum.

Figure 1 shows the simulation of distortion among the pulse laser, photon, and corrected waveforms. The laser signal is with 4.5 ns FWHM and one photoelectron intensity. The width of the time bin is 16 ps. In Fig. 1, the photon waveform moves forward, and the intensity is reduced. The waveform distortion is large between photon echo and ideal echo, whose R_C is 0.04. After correction, the R_C falls to 0.001, and the waveform almost coincides

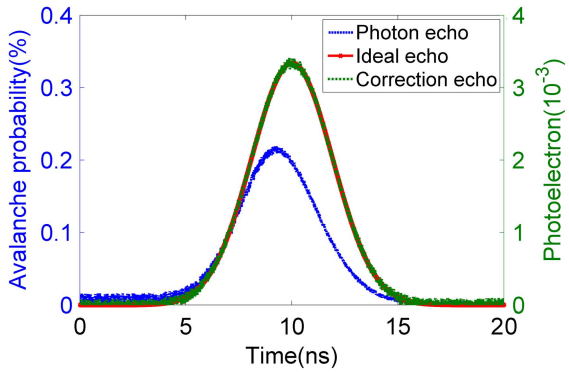

Fig. 1. Waveform distortion among the pulse laser, photon, and corrected waveforms.

with the ideal one, indicating that the correction method has a good effect.

To analyze the performance of the correction method, we compare the correlation distance and time cost with Xu *et al.*'s restoration method[27], as shown in Fig. 2. Reference [27] focuses on the single-trigger mode of photon detection and uses cumulative summation to reconstruct the target's pulsed laser echo.

Figure 2(a) shows, as the echo intensity increases, that the correlation distance increases sharply between the photon waveform and the ideal waveform. If the intensity is high, the photon waveform will move forward, and the end of the photon waveform is overwhelmed by noise. At this time, the correction method treats the end of the photon waveform as noise, resulting in the width of the corrected waveform to be similar to the pulse width of the distorted photon waveform. Therefore, the correlation distance between the corrected waveform and the ideal waveform gradually increases when the intensity increases, which is greatly less compared with the correlation distance of the photon waveform as a whole. For example, when $N_s = 3$, the R_C between the corrected waveform and the ideal waveform is 0.00184, while between the photon waveform and the ideal waveform it is 0.2571. Figure 2(b) illustrates that our method calculates much faster than that of Xu *et al.* [27], especially when the time bin width is short. The shorter the time bin width, the larger the number of time bins. Xu *et al.*'s method is the cumulative summation, and, as the number of time bins increases, the calculation time becomes longer. Meanwhile, our method does not include accumulation. Compared with that of Xu *et al.*, the calculation time of our method is increased by more than two orders of magnitude. In detail, our method costs 4×10^{-4} s less than 7×10^{-2} s of the method in Ref. [27], when the range gate is 100 ns and the time bin width is 16 ps. Therefore, our method has an obvious advantage in the restoration of full waveforms from the photon waveform and real-time analysis for the photon counting Lidar.

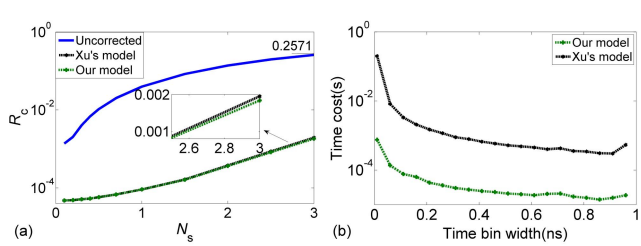

Fig. 2. Comparison with Xu *et al.*'s method. (a) Correlation distance versus the intensity; (b) time cost versus the width of the time bin.

3. Experiment Analysis

To verify the full-waveform correction method, we establish the indoor experiment system of the photon counting Lidar, as shown in Fig. 3. The width of the laser pulse is 4.5 ns, the repetition frequency is 100 kHz, and the wavelength is 1064 nm. The Geiger-mode avalanche photodiode (GM-APD) (SPD4F100A) works in the near-infrared band, and the parameters are as follows: detection efficiency of 5% at 1064 nm, dead time of 1 μs, the dark count rate of 5×10^{-6}/pulse; when the working frequency of the detector is 100 MHz, the after-pulse probability is 5%, and the time jitter is less than 400 ps. The TCSPC module (FT1040) is selected to acquire the data, and the width of the time bin is 16 ps.

A diffuse reflector is set as the target to analyze the waveform distortion and correction effect with different photon numbers. The target of 30 cm × 30 cm size is located at 5 m. By adjusting the attenuator to change the average number of echo photons, a set of experimental data is obtained. Among them, the photon waveforms and correction results with the average number of echo photons of 0.04 and 0.6 are visually shown in Fig. 4.

It can be found in Fig. 4 that there is a sudden change in the front of the photon waveform. Due to the limitation of the detector's gate, part of the echo photons cannot be detected, resulting in the loss of the front of the echo pulse. Therefore, the photon waveform changes suddenly, and the intensity of the sudden change is greater than the actual intensity. It can be seen from Fig. 1 that the laser waveform and photon waveform almost conform to the Gaussian distribution, so Gaussian fitting is used to smooth the corrected waveform. As shown in Fig. 4(a), if the average photon number is less than 0.1, the photon waveform

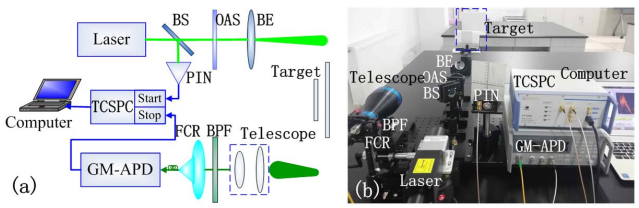

Fig. 3. Description of the photon counting system. (a) Schematic diagram: the components are a semiconductor laser source, a GM-APD detector, a TCSPC system, and the optical system. The optical system contains a beam splitter (BS), PIN fast photodiode, optical attenuation system (OAS), beam expansion (BE), telescope, bandpass filter (BPF), and fiber coupling receiver (FCR); (b) photograph of the experiment system.

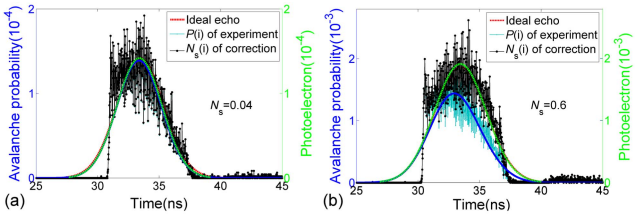

Fig. 4. Photon waveform, which is the statistical histogram from multiple cumulative detections of TCSPC and corrected waveform when (a) $N_s = 0.04$ and (b) $N_s = 0.6$. The blue line and the green line are the fitting curves of the photon waveform and the correction waveform, respectively.

and the correction waveform almost completely overlap, which can be regarded as an ideal echo waveform. As shown in Fig. 4(b), when the average photon number is large, the photon waveform moves forward with a large amplitude, and the end of the waveform is submerged in noise, with the R_C of 1.98%. After being corrected, the R_C becomes 0.22%. Not only the intensity but also the distribution of the corrected waveform is almost the same as that of the real waveform. However, it is not difficult to find that when the number of photons is large, the end of the photon distribution cannot be corrected well, and the effect of the waveform correction is weakened. To further analyze the correction effect, the correlation distance between the photon waveform and correction waveform, as well as the photon waveform and ideal waveform with varying photon numbers is shown in Fig. 5, and Table 1 shows some data.

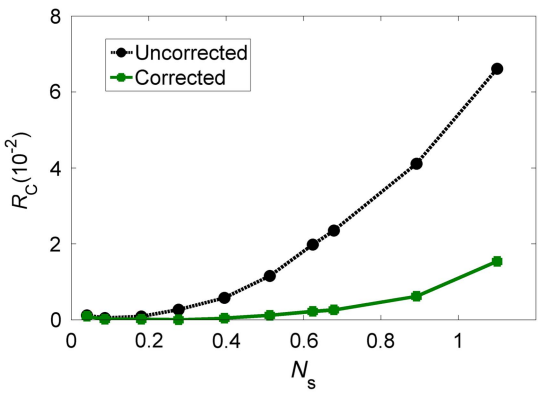

Fig. 5. Correlation distance versus the average number of photons.

Table 1. Comparison of Correction Effects with Different Echo Photon Numbers.

	N_s	0.04	0.18	0.39	0.62	0.89	1.10
R_C	Uncorrected (10^{-2})	0.05	0.09	0.58	1.98	4.11	6.61
	Corrected (10^{-2})	0.012	0.014	0.042	0.220	0.620	1.540
	Time cost (10^{-3} s)	0.37	0.39	0.42	0.36	0.43	0.38

From Fig. 5 and Table 1, it appears that with more echo photons, the correlation distance between the photon waveform and the ideal waveform increases rapidly. When the average photon number is 0.89, R_C reaches 4.11%. After the correction, R_C is reduced to 0.62%, which is a reduction of 85%. Moreover, the echo intensity has also been well corrected, and the corrected waveform can be regarded as an ideal waveform to obtain detailed information of the target. It is worth noting that the time cost of the correction method is about 0.4 ms when the gate time is 100 ns in the experiment data processing. In short, our correction method can increase the range of the average photon number intensity of photon detection, and it is conducive to rapid real-time data analysis.

To verify the effect of the correction method on the photon waveform of the target with varying depth, we conduct experiments on two targets located at 2.25 m with a distance of 1.2 m. To better describe the change of the waveform, the ratio of the pulse peak is defined as $K_I = N_{\max 1}/N_{\max 2}$, and $N_{\max k}$ is the kth peak in the echo. The relative areas of the two planes are different so that the ratios of pulse peak are 1.4 and 0.93, respectively. The results are as shown in Figs. 6 and 7.

As can be seen from Figs. 6 and 7, when the average number of echo photons is less than 0.1, the photon waveform can be regarded as the ideal waveform[12], and the correction waveform coincides with the photon waveform on the whole. As shown in Fig. 6(b), the greater the intensity, the more severe the distortion at the end of the photon waveform, and the greater the drop in intensity. In detail, when the number of photons is 0.5, the ratio of pulse peak of the photon waveform changes from 1.4 to 1.8, and the correlation distance increases from 2.78% to 6.24%. The correlation distance of the corrected waveform is slightly large because the Gaussian fitting waveform has a gap between the pulse width and the ideal pulse width. In Fig. 7(b), when the

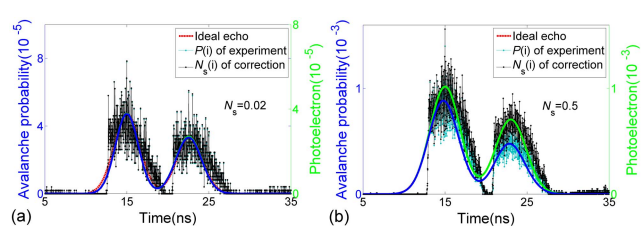

Fig. 6. Photon waveforms and correction waveforms of depth targets with (a) $N_s = 0.02$ and (b) $N_s = 0.5$ at $K_I = 1.4$.

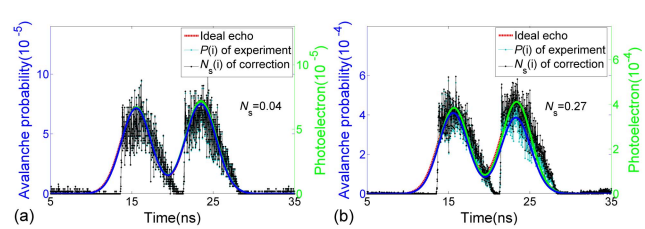

Fig. 7. Photon waveforms and correction waveforms of depth targets with (a) $N_s = 0.04$ and (b) $N_s = 0.27$ at $K_I = 0.93$.

number of photons is 0.27, the ratio of the pulse peak of the photon waveform increases from 0.93 to 1.15, the photon waveform at the end of the target with varying depth is severely distorted, and the intensity drops severely, resulting in the error of the target's information acquired from the photon waveform. After correction, the ratio of pulse peak of the corrected waveform is 0.934, which is basically equal to that of the ideal waveform. The target information in the correction waveform is more accurate. Therefore, for the target with varying depth, the full-waveform correction method can correct the photon waveform, and we can acquire the accurate target details.

4. Conclusion

In summary, a rapid universal recursive correction method of the photon waveform is proposed to restrain the distortion of the photon waveform and acquire accurate target details. The calculation time of our method is on the order of milliseconds (ms), which greatly accelerates the speed of data analysis. When the average number of echo photons is 0.89, the correlation distance is reduced by 85%, and the intensity of the correction waveform is equal to that of the actual waveform. For targets with varying depths, the signal at the end of the photon waveform is severely distorted. When the photon number is 0.27, the ratio of the pulse peak of the photon waveform increases from 0.93 to 1.15, and the corrected ratio is 0.934, which is basically equal to that of the ideal waveform. The universality of the correction method is verified. However, if the number of photons is large, the signal submerged by noise cannot be recovered due to the limitation of the external environment and the single-photon device. The correction method has an obvious advantage with the real-time analysis and accurate acquisition of target detail information for the photon counting Lidar. It is conducive to accurate analysis of the detection performance of targets hidden in vegetation or camouflaged and rapid correction of the walk error of photon ranging.

Acknowledgement

This work was supported by the National Natural Science Foundation of China (No. 61871389) and the Research Plan Project of the National University of Defense Technology (No. ZK 18-01-02).

References

1. R. E. Warburton, A. McCarthy, A. M. Wallace, S. H. Marin, R. H. Hadfield, S. W. Nam, and G. S. Buller, "Sub-centimeter depth resolution using a single-photon counting time-of-flight laser ranging system at 1550 nm wavelength," Opt. Lett. **32**, 2266 (2007).
2. L. Xue, M. Li, L. Zhang, D. Zhai, Z. Li, L. Kang, Y. Li, H. Fu, M. Ming, S. Zhang, X. Tao, Y. Xiong, and P. Wu, "Long-range laser ranging using superconducting nanowire single-photon detectors," Chin. Opt. Lett. **14**, 071201 (2016).
3. Z. Li, Q. Zhao, and W. Gong, "Performance comparison of ghost imaging versus conventional imaging in photon shot noise cases," Chin. Opt. Lett. **18**, 071101 (2020).
4. A. Kirmani, D. Venkatraman, D. Shin, A. Colaço, F. N. C. Wong, J. H. Shapiro, and V. K. Goyal, "First-photon imaging," Science **343**, 58 (2014).
5. Y. Altmann, X. Ren, A. Mccarthy, G. S. Buller, and S. McLaughlin, "Lidar waveform-based analysis of depth images constructed using sparse single-photon data," IEEE Trans. on Image Process. **25**, 1935 (2016).
6. A. M. Pawlikowska, A. Halimi, R. A. Lamb, and G. S. Buller, "Single-photon three-dimensional imaging at up to 10 kilometers range," Opt. Express **25**, 11919 (2017).
7. J. Qiao, F. Mei, and Y. Ye, "Single-photon emitters in van der Waals materials," Chin. Opt. Lett. **17**, 020011 (2019).
8. Z. P. Li, X. Huang, P. Y. Jiang, Y. Hong, C. Yu, Y. Cao, J. Zhang, F. H. Xu, and J. W. Pan, "Super-resolution single-photon imaging at 8.2 kilometers," Opt. Express **28**, 4076 (2020).
9. Y. Kang, L. F. Li, D. W. Liu, D. J. Li, T. Y. Zhang, and W. Zhao, "Fast long-range photon counting depth imaging with sparse single-photon data," IEEE Photonics J. **10**, 7500710 (2018).
10. Z. P. Li, X. Huang, Y. Cao, B. Wang, Y. H. Li, W. J. Jin, C. Yu, J. Zhang, Q. Zhang, C. Z. Peng, F. H. Xu, and J. W. Pan, "Single-photon computational 3D imaging at 45 km," Photonics Res. **8**, 1532 (2020).
11. M. Henriksson, H. Larsson, C. Groenwall, and G. Tolt, "Continuously scanning time-correlated single-photon-counting single-pixel 3-D lidar," Opt. Eng. **56**, 031204 (2017).
12. X. M. Ren, "Advanced photon counting techniques for long-range depth imaging," Ph.D Dissertation (Heriot-Watt University, 2015).
13. W. Becker, *Advanced Time-Correlated Single Photon Counting Techniques* (Springer Science & Business Media, 2005).
14. A. M. Wallace, Y. Jing, K. J. Nils, M. C. Aongus, J. C. Robert, and S. B. Gerald, "Full waveform analysis for long-range 3D imaging laser radar," EURASIP J. Adv. Signal Process. **2010**, 896708 (2010).
15. Y. Altmann, X. M. Ren, A. Mccarthy, G. S. Buller, and S. McLaughlin, "Robust bayesian target detection algorithm for depth imaging from sparse single-photon data," IEEE Trans. Comput. Imaging **2**, 456 (2016).
16. T. G. Yin, N. Lauret, and J. P. Gastellu-Etchegorry, "Simulation of satellite, airborne and terrestrial LiDAR with DART (II): ALS and TLS multi-pulse acquisitions, photon counting, and solar noise," Remote Sens. Environ. **184**, 454 (2016).
17. B. C. Du, Z. H. Li, G. Y. Shen, T. X. Zheng, H. Y. Zhang, L. Yang, and G. Wu, "A photon-counting full-waveform lidar," Chin. Phys. Lett. **36**, 094201 (2019).
18. O. Steinvall, "Effects of target shape and reflection on laser radar cross sections," Appl. Opt. **39**, 4381 (2000).
19. O. Steinvall and M. Tulldahl, "Laser range profiling for small target recognition," Opt. Eng. **56**, 031206 (2017).
20. O. Steinvall, S. Lars, M. Henriksson, and P. Jonssson, "High resolution ladar using time-correlated single-photon counting," Proc. SPIE **6950**, 695002 (2008).
21. R. A. Barton-Grimley, J. P. Thayer, and M. Hayman, "Nonlinear target count rate estimation in single-photon lidar due to first photon bias," Opt. Lett. **44**, 1249 (2019).
22. A. Hou, Y. Hu, N. Zhao, J. Fang, S. Xu, and X. Zhang, "Full-waveform distortion characteristics of photon counting lidar at different dead-time," Optik **223**, 165448 (2020).
23. M. S. Oh, H. J. Kong, T. H. Kim, K. H. Hong, and B. W. Kim, "Reduction of range walk error in direct detection laser radar using a Geiger mode avalanche photodiode," Opt. Commun. **283**, 304 (2010).
24. W. He, B. Sima, Y. Chen, H. Dai, Q. Chen, and G. Gu, "A correction method for range walk error in photon counting 3D imaging lidar," Opt. Commun. **308**, 211 (2013).
25. Z. Chen, X. Li, X. Li, G. Ye, Z. Zhou, L. Lu, T. Sun, R. Fan, and D. Chen, "A correction method for range walk error in time-correlated single-photon counting using photo-multiplier tube," Opt. Commun. **434**, 7 (2019).
26. K. Huang, S. Li, Y. Ma, X. Tian, H. Zhou, and Z. Zhang, "Theoretical model and correction method of range walk error for single-photon laser ranging," Acta Phys. Sin. **67**, 064205 (2018).
27. L. Xu, Y. Zhang, Y. Zhang, L. Wu, C. Yang, X. Yang, Z. Zhang, and Y. Zhao, "Signal restoration method for restraining the range walk error of Geiger-mode avalanche photodiode Lidar in acquiring a merged three-dimensional image," Appl. Opt. **56**, 3059 (2017).

28. P. Jonsson, M. Tulldahl, J. Hedborg, M. Henriksson, and L. Sjöqvist, "Experimental evaluation of penetration capabilities of a Geiger-mode APD array laser radar system," Electron. Opt. Remote Sens. **10**, 1043405 (2017).
29. J. J. Degnan, "Photon-counting multi-kilohertz micro-laser altimeters for airborne and space-borne topographic measurements," J. Geodyn. **34**, 503 (2002).
30. S. Johnson, P. Gatt, and T. Nichols, "Analysis of Geiger-mode APD laser radars," Proc. SPIE **5086**, 359 (2003).
31. P. Gatt, S. Johnson, and T. Nichols, "Geiger-mode avalanche photodiode LADAR receiver performance characteristics and detection statistics," Appl. Opt. **48**, 3261 (2009).
32. M. S. Oh, H. J. Kong, T. H. Kim, K. H. Hong, B. W. Kim, and D. J. Park, "Multi-hit mode direct-detection laser radar system using a Geiger-mode avalanche photodiode," Rev. Sci. Instrum. **81**, 033109 (2010).
33. Z. Li, J. Lai, C. Wang, W. Yan, and Z. Li, "Influence of dead-time on detection efficiency and range performance of photon-counting laser radar that uses a Geiger-mode avalanche photodiode," Appl. Opt. **56**, 6680 (2017).